Recent Dynamical Relaxation of Galaxy Clusters: Evidence for a Low-Ω_m Universe

Adrian L. Melott[1,3], Scott W. Chambers[1], and Christopher J. Miller[2]

[1]Dept. of Physics & Astronomy, Univ. of Kansas, Lawrence, KS 66045

[2]Dept. of Physics & Astronomy, Carnegie Mellon Univ., Pittsburgh, PA 15213

[3]melott@kusmos.phsx.ukans.edu

ABSTRACT

We argue that there has been substantial evolution in the ellipticity of rich galaxy clusters between $0 < z < 0.1$, and suggest that this is additional evidence for a low matter-density Universe.

Subject headings: cosmology: large-scale structure of universe – galaxy clusters: evolution

1. Introduction

Clusters of galaxies are often elongated systems (Carter & Metcalfe 1980) whose shapes and orientations are described by (projected) ellipticities and position angles. Dynamical and cosmological information can be inferred from these rather general parameters. For example, position angles show clusters are generally aligned with neighboring rich clusters, as suggested by projected galaxy distributions (Binggeli 1982; Rhee, van Haarlem & Katgert 1992; Plionis 1994) and X-ray isophotal morphologies (*e.g.* West, Jones & Forman 1995; Chambers, Melott & Miller 2000, 2001). Clusters tend to be aligned along these axes as a relic of gravitational clustering. However, if the flow slows greatly, as it will in a low-density Universe, clusters will have time to relax to a more spherical shape (e.g. Tsai & Buote 1996; Buote 1998). In a high-density cosmological background, mergers continue, preventing the clusters form relaxing.

We investigate whether galaxy cluster ellipticity has evolved significantly in recent cosmological times ($0 < z < 0.1$). Clusters experiencing recent mergers will likely appear more elongated than relaxed clusters.

2. Formulating The Null Hypothesis and Analysis

In examining data related to the question of cluster alignment (Chambers, Melott, and Miller 2001) we noticed that most of the signal for alignment came from redshifts $z > 0.06$. We did not expect that this could be due to incompleteness, since the surveys used there (MX Northern Abell Cluster Survey: Slinglend *et al.* 1998; ESO Nearby Abell Cluster Survey: Katgert *et al* 1996) are 98% complete in redshift measurements for Abell/ACO clusters of richness $R \geq 1$ for redshifts $0 < z < 0.1$. Additionally, the number density as a function of redshift is flat out to $z = 0.1$ (Miller & Batuski 2001). Furthermore, in that study we carefully compensated for any selection biases caused by the smaller volume at low z by excluding from consideration any cluster whose nearest neighbor was more distant than the nearest boundary of the survey region. This assures that a "true" nearest neighbor is not missed, lying just outside the sample.

One of the obstacles in alignment studies is random error in the assignment of the position angle. If clusters had relaxed and become more nearly spherical at cosmologically recent times, there would be correspondingly greater ambiguity in the assignment of the axes. Our null hypothesis is therefore that cluster ellipticity does not increase with increasing redshift. The simplest approach with our two variables is to ask whether there is a correlation between ellipticity and redshift. The linear correlation coefficient tests for this

and may be cast in the form

$$r = \frac{\Sigma(\epsilon_i - \overline{\epsilon})(z_i - \overline{z})}{\Sigma[(\epsilon_i - \overline{\epsilon})^2 (z_i - \overline{z})^2]^{1/2}} \quad (1)$$

where the sum is over all i, and $\overline{\epsilon}$ and $\overline{z}$ are the mean ellipticity and redshift, respectively.

3. Sample Selection

There are a number of issues that must be accounted for when creating samples to be used in this analysis. First, the base cluster catalog must show evidence for being complete within the volume studied. This catalog must also contain a large number of well-defined clusters over a large portion of the sky. Projection effects need to be minimized, and multi-wavelength data is a necessity. Fortunately, the Abell/ACO catalog meets all of these requirements. The current redshift data for Abell/ACO clusters extends beyond $z = 0.1$, covering half of the sky (see e.g. Slinglend et al. 1998; Miller & Batuski 2001). If we restrict our catalog to the richest Abell/ACO clusters, we can minimize optical projection effects (Miller et al. 1999a,b). A large number of Abell/ACO clusters have X–ray data, which can also be used to avoid projection effects. There is substantial evidence that these clusters are free of selection biases and that they are a biased representation of the luminous mass distribution (Miller et al. 1999a; Miller & Batuski 2001).

In order to reduce selection biases and assure accurate redshifts for our sample, we excluded any clusters which not were present in the range $0.012 < z < 0.1$ and galactic latitude $|b| \geq 30^o$. We made a richness cut requiring $R \geq 1$ as specified in Abell (1958) or Abell, Corwin, and Olowin (1989). This richness cut limits our studies to the most massive and easily detected clusters. However, $R = 0$ clusters were never meant to be treated as a complete sample of clusters and there are too many that are mis-identified or un-identified, and so we exclude this subset entirely. We place a minimum physical size within which ellipticities are calculated at $1h^{-1}$Mpc. This is less than the "typical" Abell radius of $1.5h^{-1}$Mpc, but still large enough to map the outer regions of clusters which are most affected by infall. The inner isophotes of clusters are known to be less sensitive to the cosmological background from simulations (Evrard 2001) and data (West & Bothun 1990, hereafter WB). We excluded any study having a circular "mask" within which counts or measurements were made with radius < 1 Mpc/h. Examples of such excluded datasets from the literature include those of Carter & Metcalfe (1980) and Binggeli (1982). Binggeli notes that these methods systematically underestimate ellipticity.

Rhee, van Haarlem & Katgert (1991; RvHK hereafter) studied 107 rich $R \geq 1$ cluster at $z < 0.1$. Using various methods, they measured the ellipticity determined from galaxies

within a radius $\sim$ 1-2 h^{-1}Mpc of the cluster center. We employ this sample, using the ellipticity measured by tensor method (RvHK). The Kolokotronis et al. 2001 (KBPG) study of 22 rich cluster optical and X-ray images showed that their shape parameters are generally correlated. Their optical sample used a moments method on APM galaxies within r $\sim$ 1.8 h^{-1}Mpc of the cluster center to determine the ellipticity. We also adopt this optical sample. WB used a smoothing technique to assign ellipticities to $\sim$ 70 clusters in a substructure study. We use the ellipticities determined from the outer regions in this study.

The use of X-ray samples is extremely important, due to a greatly reduced possibility of projection effects contaminating ellipticity measurements. Fewer X-ray samples are available. We use the McMillan, Kowalski & Ulmer (1989; MKU) sample of 49 *Einstein* X-ray clusters. In their method, the outer regions of the cluster was emphasized. We also study the KBPG sample of 22 ROSAT ellipticities, which focused on the central region of the clusters. Central regions tend to be rounder and therefore contribute large random error to shape parameters. However, KBPG demonstrated that the shape parameters from their optical and X-ray images are correlated. Although the correlation is not strong, we adopt their X-ray sample as a cross-check with the optical sample. Again, we excluded any estimates of ellipticity based only on regions with a radius $<$ 1 Mpc/h. Plionis et al. (1991) described ellipticity evolution, but did not include any X-ray data.

After being filtered through the richness, redshift, and galactic latitude requirements described earlier, the RvHK optical sample is our largest sample with 96 clusters. The MKU X-ray sample of 30 surviving clusters is the next largest. WB reduces to 25 and KBPG to 18 clusters. Later, WB will reduce further as ellipticities are not given for all clusters.

4. Analysis and Results

We wish to determine whether ellipticity is positively correlated with redshift. To this end, we test our samples for linear correlation (Bevington and Robinson 1992). The correlation coefficient, r has a range of values $-1 < r < 1$. If $|r|$ is close to 1, the data are strongly correlated. If r=0 the data are uncorrelated. We therefore expect $r > 0$ if clusters are more elliptical at higher redshifts, r=0 if there is no change, and $r < 0$ if ellipticity decreases with redshift. We have not merged the samples because of apparent systematic differences in ellipticity assignment. Authors used different methods to measure ellipticity. WB systematically excluded ellipticities which they did not conclude were significant, and we see systematically larger ellipticities with a strong redshift gradient. Merging samples with very different mean ellipticities may falsely kill or intensify the signal. We have,

however, converted all ellipticities given to the same notation,

$$\epsilon = 1 - \frac{b}{a} \tag{2}$$

where a is the projected major axis and b is the projected minor axis. We note that we are dealing with projections and that intrinsically more spherical systems will more often appear circular in projection (Plionis et al. 1991).

The results of the correlation statistic are given in Table 1. Included is the sample name, number of clusters, N_{cl}, and the correlation coefficient, r. The last column contains the probability P that the correlation coefficient could arise from an uncorrelated sample. The confidence is 1 - P. Interestingly, for all samples, r is positive, ranging from 0.22 to 0.67, indicative of cluster ellipticity being an increasing function of redshift. The range of values reflects systematic differences in the samples.

MKU are the only authors to provide errors on their ellipticities. For consistency, we have given in the table an unweighted r. However, the error-weighted r for this sample is 0.39, essentially the same as the unweighted. The WB sample has the largest correlation coefficient with highest confidence. The ellipticities in the WB sample are higher and increase more rapidly with redshift than the other samples. This, and the small scatter in the data, results in WB's strong signal. We note that WB applied considerable smoothing to cluster profiles, and rejected any results with high uncertainty, when computing ellipticities. In Figures 1 & 2 we plot the ellipticity vs. redshift for the X-ray and optical samples, respectively. The increase with redshift is apparent. It is noteworthy that the increasing trend exists in all X-ray and optical samples.

5. Possible Sources of Systematic Error

We cannot exclude some type of systematic error as the source of this signal. However, we have removed some of the more obvious possibilities by keeping only those clusters which are members of a carefully controlled volume-limited sample and by using both optical and X-ray samples. Our results depend on accurate measurements of the cluster ellipticities. Confirmation of our results will be possible using upcoming controlled cluster catalogs from the Sloan Digital Sky Survey (SDSS) (e.g. Kim et al. 1999; Annis et al. 1999). The five color photometry of the SDSS data will enable accurate ellipticity calculations for clusters to $z \sim 0.4$ (see Kim et al. 2000).

In the meantime, we can address some more obvious effects which may lead to a false signal. For instance, clusters of a fixed physical size at higher redshift are smaller in

angular size. It is therefore more difficult to measure ellipticities as they appear on the sky. However, at our redshift limit of $z = 0.1$, a typical cluster diameter is still $\sim 20 - 30$ arc-minutes. Therefore, ellipticity measurements should not be unduly difficult within our specified redshift range.

Another possible source of contamination that could affect our samples is redshift bias in the distribution of cooling flow (CF) clusters. Cooling flow clusters tend to be more relaxed and spherical in the X-ray but need not be so in the optical (Henriksen 1993). Thus we need to address the possibility that our X-ray samples could be biased if the distribution of CF clusters were biased by redshift. Using the compilation from Loken, Melott, and Miller (1999), we find that the number of identified cooling flow clusters within our X–ray samples is 40% and 17% for the MKU and KBPG samples respectively. We performed a Kolmogorov-Smirnov test on the distribution of redshifts for the MKU cooling flow clusters versus the total sample and find no significant difference. In fact, the K-S test indicates a 95% probability that the distribution of CF clusters in the MKU sample could have been drawn from the parent population of that entire sample. The KBPG contains too few cooling flow clusters to perform a K-S test. However, the three KBPG cooling flow clusters have redshifts z=0.046, 0.0602, and 0.0750, and so they cannot be contributing to our signal.

We excluded clusters for which WB conclude the ellipticity is not measurable due to large error. A large fraction of these unmeasurable clusters at our redshift limits could also induce a false signal. WB do not specify errors or their exact procedure for rejecting ellipticities. The 7 clusters excluded out of 25 which survived our cuts are at small to moderate redshift. We assess the significance of their culling by re-introducing the rejected clusters with mock ellipticities. If we assign them ellipticities equal to the mean in their redshift bin (binsize 0.01) for all the other samples, r increases to 0.79 with a probability of no correlation $< 1e - 8$. If we assign them ellipticities equal to the mean of the WB for all redshifts, r decreases to 0.40 with a probability of $4e - 2$. The latter procedure would mimic the effect if they had systematically excluded clusters with high ellipticity at moderate redshift.

There are, of course, other biases that could exist, such as in the luminosity selection of the subsamples. We note that de Theije et al. (1995) in a re-analysis of ellipticity studies, argue that most methods underestimate large ellipticities, and overestimate small ones, so that the evolution could be even faster than we have measured. They did not include WB in this study. Differences in methods could account for the differences in r values between various samples used here.

6. Discussion

The hypothesis of evolving ellipticity was formulated on a simple physical basis. Perturbations are typically highly anisotropic when they first collapse (Shandarin et al. 1995). Gravitational clustering in the nonlinear regime results in the flow of matter along filaments and sheets to form clusters (Shandarin and Klypin 1994). These clusters would then become part of a larger-scale flow and merging to produce even larger objects (Pauls and Melott 1995).

Once the clusters are essentially collapsed along all 3 axes, relaxation can begin. Gravitational relaxation is well-understood to move toward isotropizing the system. Thus, if the clusters were isolated, they would become more spherical (circular in projection).

In a high-density Universe, mergers are expected to continue to the present time. In a low-Ω_m Universe, with or without a cosmological constant, linear gravitational clustering shuts down as the matter density declines (Peebles 1980; Lahav et al. 1991; Hamilton 2001).

If clustering continues unabated, new mergers and infall of matter along filaments will tend to keep clusters aspherical. If linear clustering shuts down, mergers will tend to run out of fuel after existing bound objects have completed their infall. Our signal for ellipticity evolution is additional evidence for the kind of isolation and relaxation of clusters that will be characteristic of a low-density Universe.

Is the timescale reasonable? Relaxation can take place as a consequence of the time-dependent gravitational potential which varies on a crossing time. It is therefore appropriate to compare the crossing time for clusters to the time over which we observe evolution.

The crossing time for a galaxy in a cluster is

$$t_{cross} \sim (\frac{R}{1Mpc})(\frac{1000km/s}{\sigma_v})Gyr. \quad (3)$$

where R is the radius in Mpc and σ_v is the line of sight velocity dispersion in km/s. This can be compared with the roughly 1.3 Gyr timescale for our sample, assuming h=0.7, q_0=0. This interval is also comparable to the time gas remains in dis-equilibrium after having been stripped by the merger of two groups (Evrard 1990).

Further supporting evidence comes from an analysis of the Butcher-Oemler effect (Ellingson et al. 2001) arguing that the effect is dominated by a redshift-dependent number of blue galaxies in clusters, which are primarily located in the outer regions of these clusters, and show dramatic declines in infall rates. Wang & Ulmer (1997) note a strong correlation between cluster ellipticity and blue fraction, further supporting this connection.

Our data have too much scatter to justify going beyond linear order. Future work with larger, more uniform samples may enable a detailed comparison with theory and ellipticity evolution in simulations. In particular, we look forward to testing this result against (1) X-ray selected cluster samples sensitive to extended emission (2) Optically selected catalogs based on new selection techniques which will produce even more uniform samples, based on surveys such as SDSS and 2dF (York et al. 2000; Davis & Newman 2001).

7. Acknowledgments

We are grateful for support from the NSF under grant number AST-0070702, as well as useful comments from the referee Andrew Hamilton.

REFERENCES

Abell, G.O. 1958, ApJS, 3, 211

Abell, G.O., Corwin Jr., H.G., Olowin, H.G., 1989, ApJS, 70, 1

Annis, J., Kent, S., Castander, F., Eisenstein, D., Gunn, J., Kim, R., Lupton, R., Nichol, R., Postman, M., Voges, W., SDSS Collaboration 1999, American Astronomical Society Meeting, 195, 1202

Bevington, P.R., & Robinson, D.K. 1992, Data Reduction and Error Analysis for the Physical Sciences, New York, McGraw-Hill

Binggeli, B. 1982, A&A, 107, 338

Buote, D.A. 1998, MNRAS, 293, 382

Carter, D., and Metcalfe, N. 1980, MNRAS, 191, 325

Chambers, S.W., Melott, A.L., Miller, C.J. 2000, ApJ, 544 104

Chambers, S.W., Melott, A.L., Miller, C.J. 2001, submitted to ApJ

Davis, M., & Newman, J. 2001 preprint astro-ph/0104418

de Theije, P.A.M., Katgert, P., & van Kampen, E. 1995 MNRAS 273, 30

Ellingson, E., Lin, H., Yee, K.C., & Carlberg, R.G. 2001 ApJ, 547, 609

Evrard, A. 1990 in Clusters of Galaxies (STScI Symposium 4) Cambridge Univ. Press p287

Evrard, A. 2001, personal communication.

Hamilton, A.J.S. 2001, MNRAS, 322, 419

Henriksen, M.J. 1993, ApJ, 407, L13

Katgert, P., et al. 1996, A&A, 310, 8

Kim, R. S. J., Strauss, M. A., Postman, M., Kepner, J. V., Bahcall, N. A., Gunn, J. E., Lupton, R. H., Voges, W., Vogeley, M. S., SDSS Collaboration 1999, American Astronomical Society Meeting, 195, 3003

Kim, R.S.J. 2000 Ph.D. Thesis

Kolokotrinis, V., Basilakos, S., Plionis, M., Georgeantopoulos, I. 2001, MNRAS, 320, 49

Lahav, O., Rees, M.J., Lilje, P.B., Primack, J.R. 1991, MNRAS, 251, 128

Loken, C., Melott, A.L, & Miller, C.J. 2001 ApJ, 520L,5L

McMillan, S.L.W., Kowalski, M.P., Ulmer, M.P. 1989, ApJS, 70, 723

Miller, C., & Batuski, D. 2001 ApJ, 551,635

Miller, C.J., Batuski, D.J., Slinglend, K.A., and Hill, J.M. 1999 ApJ 523, 492

Miller, C.J., Krughoff, K.S., Batuski, D.J., Slinglend, K.A.,& Hill, J.M. 2000, submitted to AJ

Miller, C.J., Ledlow, M.J. & Batuski, D.J. 1999, MNRAS, submitted, astro-ph/9906423

Pauls, J.L., Melott, A.L. 1995, MNRAS, 274, 99

Peebles, P.J.E. 1980 The Large-Scale Structure of the Universe, Princeton, Princeton University Press

Plionis, M., Barrow, John. D, & Frenk, C.S. 1991 MNRAS, 249, 662

Plionis, M. 1994, ApJ, 95, 401

Rhee G.F.R.N., van Haarlem M., Katgert P. 1991, A & A Supp., 91, 513

Rhee G.F.R.N., van Haarlem M., Katgert P. 1992, AJ, 103, 1721

Shandarin, S.F., and Klypin, A.A., 1984, Sov Astron. 28, 491

Shandarin, S.F., Melott, A.L., McDavitt, K., Pauls, J.L., & Turner, J. 1995, Phys.Rev.Lett., 75, 7

Slinglend, K., Batuski, D., Miller, C., Haase, S., Michaud, K., & Hill, J. 1998, ApJS, 115, 1

Tsai, J.C., Buote, D.A. 1996, MNRAS, 282, 77

Wang, Q,D., & Ulmer, M. 1997, MNRAS, 292, 920

West, M.J., Bothun, G.D. 1990, ApJ, 350, 36

West M.J., Jones C., Forman W. 1995 ApJ, 451, L5

York, D. G. et al. 2000, AJ, 120, 1579

Table 1. Ellipticity-Redshift Correlation

Sample		N_{cl}	r	Prob.
KBPG	opt.	18	0.59	2 e -3
KBPG	xray	18	0.31	1 e -1
MKU	xray	30	0.41	9 e -3
RvHK	opt.	96	0.22	1.4 e -2
WB	opt.	18	0.67	1.5 e -4

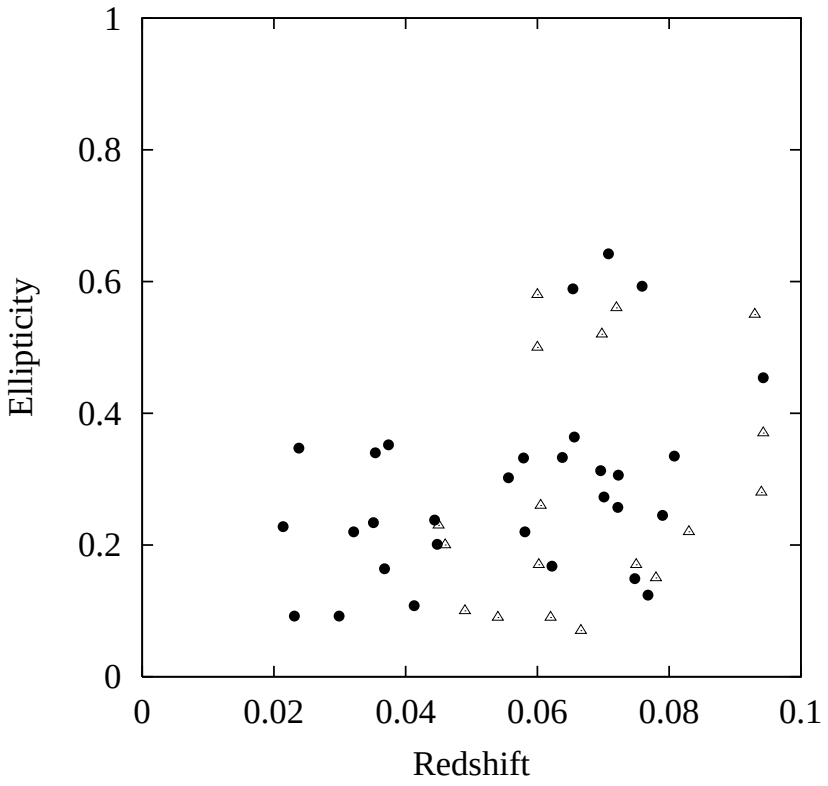

Fig. 1.— Ellipticity vs. redshift for X-ray samples. Filled circles represent MKU data; empty triangles are KBPG.

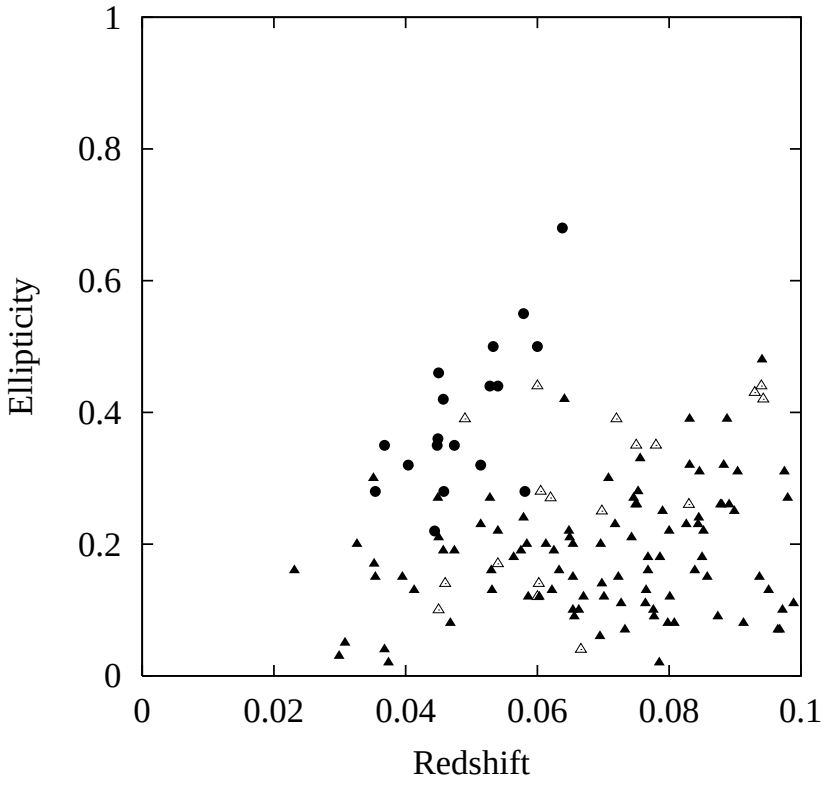

Fig. 2.— Ellipticity vs. redshift for optical samples. Filled circles are WB data; filled triangles are RvHK data; empty triangles are KBPG.